SIMULATION OF THE BEHAVIOR OF PROTOTYPES OF ROCKFILL DAMS DURING OVERTOPPING SCENARIOS. SEEPAGE EVOLUTION AND BEGINNING OF FAILURE

Joint theme between:

CIMNE

(International Center for Numerical Methods in Engineering)
Antonia Larese De Tetto   Riccardo Rossi   Eugenio Oñate

Polytechnic University of Madrid
Miguel Ángel Toledo   Rafael Moran   Hibber Campos,

CEDEX

Centre for Hydrographical Studies
Angel Lara   Mª del Pilar Viña

TABLE OF CONTENTS

LIST OF TABLES

LIST OF FIGURES

INTRODUCTION

In recent years the technology on embankments dams has developed sensibly due to the advances in soil mechanic, and in all related sciences. Nevertheless their vulnerability to overtopping still remains their weakest point in comparison with concrete structures.
The principal aim of this theme is the simulation of the initial stage of failure of the dam when an overtopping or an exceptional flood occurs.
A fluid-structure coupled problem has to be considered.
The sudden variation of the upstream conditions induces a quick evolution of a seepage line in the downstream shoulder. Non linear Darcy law has to be taken into account.
On the other hand the water, emerging from the toe of the dam, induces dragging of particles and possible mass sliding, depending on geometrical and material conditions.
UPM and CEDEX have carried out more than 70 experiments during the last two years. They analyzed the influence of a series of parameters on the failure mechanisms. These parameters are, for instance, the dimension of the rocks, the slope of the downstream part of the dam, the type of impermeable element used, and so on.
We propose to reproduce numerically three experiments analyzing the evolution of seepage and following initial stage of failure in the case of a homogeneous dam, of a dam with impermeable upstream face and of a dam with internal core. Experimental data, bottom pressure distribution and topographic analysis of the geometry of the dam during the failure can be compared with numerical results.

EXPERIMENTAL SETTINGS AND MEASUREMENTS

UPM and CEDEX have been developing more than 70 experiments in thee last years to study deeply the phenomenon of overtopping in embankments dams focusing particularly on its initial phase, when the first breach appears in the downstream slope leading eventually to a complete failure.
For each experiment a sequence of incremental discharges is imposed. Every step (characterized by a value of incoming discharge) is analyzed when the stationary regime is reached. Bottom pressure distribution is measured. When partial failure of the downstream slope or movement of the same appears, a stabilization of the failure mechanism is achieved before calculating the bottom pressure distribution and the advance degree of failure with the help, in some cases, of a photogrammetric analysis of the new downstream slope stable configuration. The experiment ends when the failure of the dam is complete.

Instrumentation

Pressure sensors are inserted in the bottom of the experimental channels. In the case of the channel of case A and B, the UPM channel, the pressure sensors are 84. They are uniformly distributed in the bottom of the dam along 7 parallel lines as described in Case A and B sections. In the case of CEDEX channel (case C) the pressure sensors are 44. Their distribution will be detailed later on.
Pressure values at the stationary regime are read on millimetric panels (see Figure 1).

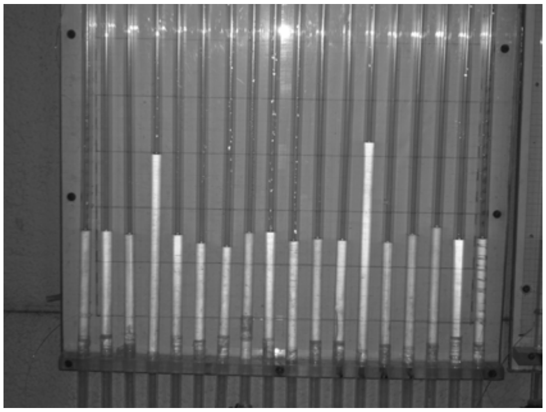

a) One of the panel for reading pressure heights.

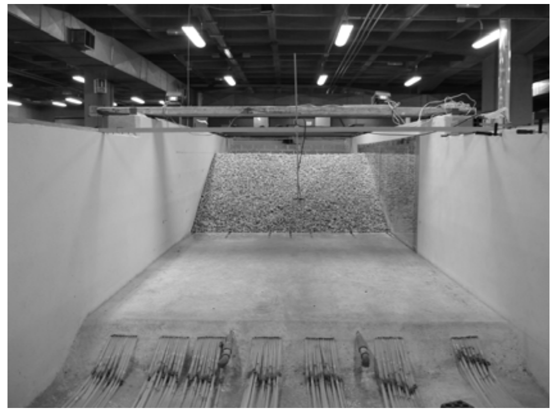

b) Front view of the channel with the pressure sensor tubes

Figure 1. Pressure instrumentation.

Topographic analysis of slope failure

The formation of the first breaches and their evolution are analyzed at each discharge step. When the stationary regime is achieved and the stable configuration of the slope is reached, the advance degree of failure (B in Figure 2a) is measured. It is by definition, the horizontal projection of the distance between the original downstream toe line and the higher point of the failed area. Colored strikes on the initial slope, help the measurement of B (see Figure 2b for an example).

In some of the experiments (case A for instance), a more detailed measurement of B is performed using a *close-object-photogrammetry-technique*. It consists on taking a series of photos in a very short time interval and continuing this sequence of photos till the end of the simulation. Through the re-elaboration of this data the creation of a digital model of the slope geometry evolution is possible and the dynamic failure is followed with high precision (see for instance Figure 3).

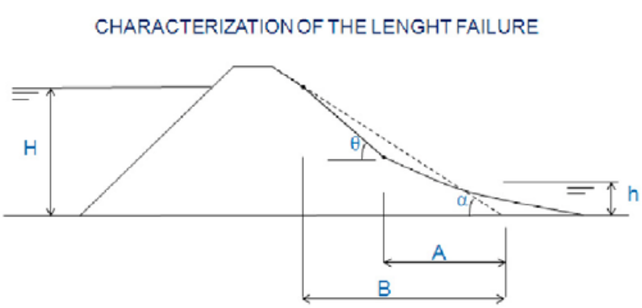

a) Schematic view of the length of failure B.

b) Visual measurement of the advance degree of failure with the help of coloured lines

Figure 2. Length of failure. Characterization and operative measurement.

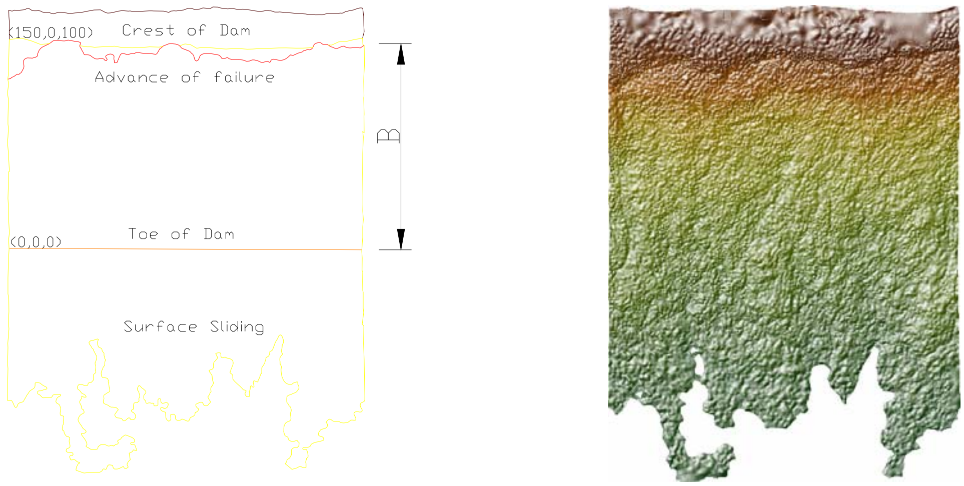

Figure 3. Digital model of the slope to evaluate the advance degree of failure B.

BENCHMARKS TESTS

The aim of this theme is the study of the structural response of a rockfill experimental dam for a given incoming/overtopping discharge.
Three different test-cases will be proposed:

- **Case A.** A homogeneous dam;
- **Case B.** A dam with internal core (simulation only of the downstream shoulder).
- **Case C.** A dam with upstream impermeable face;

For each case i (i = A, B or C), two sub analyses are proposed:

- **Case i.1** Analysis of non linear seepage given an incoming/overtopping discharge.
  Bottom pressure values at the stationary regime are provided.

- **Case i.2** Analysis of the evolution of failure given an incoming/overtopping discharge.
  Bottom pressure values together with the measurements of the advance degree of failure at the stationary regime are provided for each experimental discharge.
  Three different values of discharges are considered in this case.
  Case i.2.j+1 has as initial configuration the final solution of **Case i.2.j** in terms of pressure and advance degree of failure.

Every sub case is characterized by a different upstream discharge. A summary of all the cases presented is given in Table 1.

	CASE A Homogeneous Dam	**CASE B** Core Dam	**CASE C** Dam with impermeable face
WITHOUT FAILURE Non linear seepage evolution analysis	A.1 Q=25.46l/s	B.1 Q=5.93l/s	C.1 Q=5.17l/s
WITH FAILURE Failure evolution analysis	A.2.1 Q=51.75l/s A.2.2 Q=69.07l/s A.2.3 Q=90.68l/s	B.2.1 Q=19.36l/s B.2.2 Q=30.45l/s B.2.3 Q=39.56l/s	C.2.1 Q=15.36l/s C.2.2 Q=25.05l/s C.2.3 Q=30.27l/s

Table 1. Summary of the upstream discharges for each considered case study.

CASE A) HOMOGENEUS DAM

The first case study is a homogeneous dam. Although this kind of structure is radically different from a real dam, the study of the evolution of seepage and initial formation of breaching is very interesting. No overtopping can be reached in this case, the complete failure of the dam occurs before the overtopping discharge can be achieved. The experiment was performed by UPM.

Geometry and material

The granular material used in this experiment is homogeneous and has the following characteristics:

Porosity	= 0.4052;
Pore index	= 0.68;
Apparent specific weight	= 2.50 gr/cm^3
Dry density	= 1.49 gr/cm^3
Saturated density	= 1.91 gr/cm^3
D_{50}	= 35.04mm.

The experimental setting is a channel of the UPM laboratories. The length of the channel is 13.535m, its width is 2.46m and its height is 1.31m. All details about the initial geometry of the channel and of the dam can be found in Figure 4.

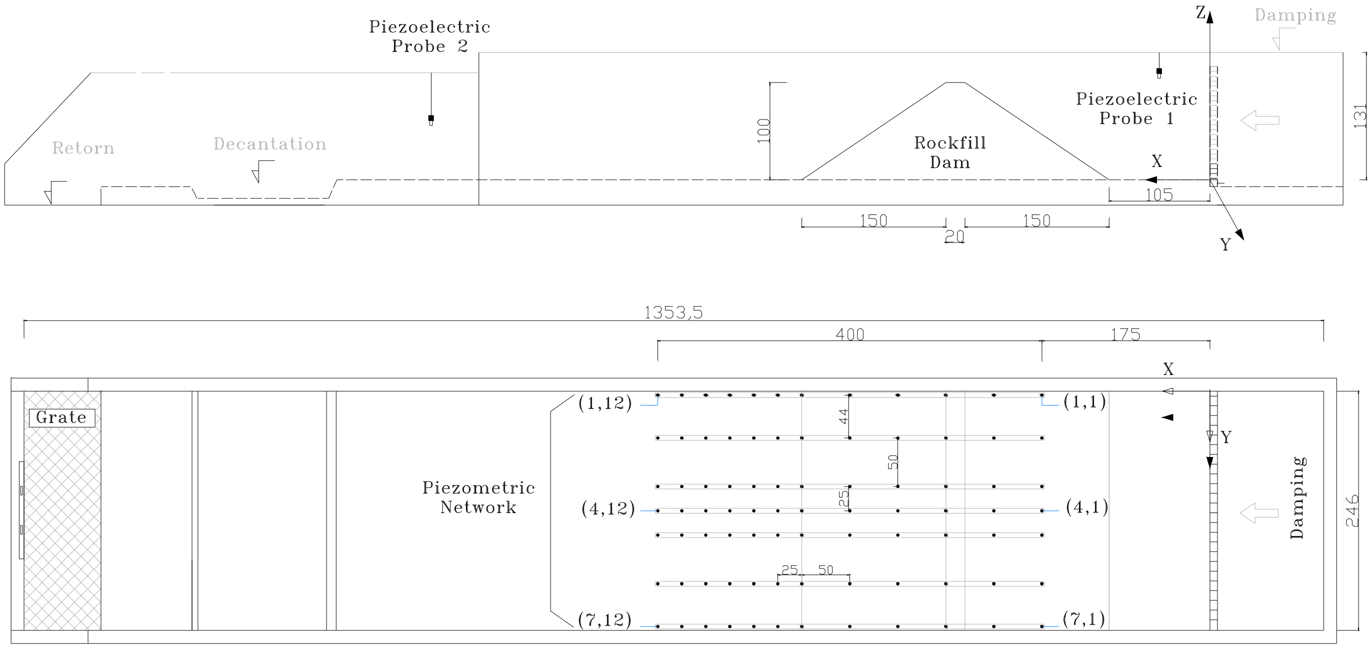

Figure 4. Case A. Geometry of the experimental setting of the homogeneous dam and pressure sensor distribution.

Figure 5. Case A. Some photos of the experimental channel and of and homogeneous dam

Pressure measurements are performed through a red of 36 sensors positioned at the bottom of the channel. They are distributed along three longitudinal lines. The detailed position of the sensors is reported in Table 2.

Sensor	X position (cm)	Y position (cm)
S (1,1)	175	4
S (1,2)	225	4
S (1,3)	275	4
S (1,4)	325	4
S (1,5)	375	4
S (1,6)	425	4
S (1,7)	450	4
S (1,8)	475	4
S (1,9)	500	4
S (1,10)	525	4
S (1,11)	550	4
S (1,12)	575	4

Sensor	X position (cm)	Y position (cm)
S (4,1)	175	123
S (4,2)	225	123
S (4,3)	275	123
S (4,4)	325	123
S (4,5)	375	123
S (4,6)	425	123
S (4,7)	450	123
S (4,8)	475	123
S (4,9)	500	123
S (4,10)	525	123
S (4,11)	550	123
S (4,12)	575	123

Sensor	X position (cm)	Y position (cm)
S (7,1)	175	242
S (7,2)	225	242
S (7,3)	275	242
S (7,4)	325	242
S (7,5)	375	242
S (7,6)	425	242
S (7,7)	450	242
S (7,8)	475	242
S (7,9)	500	242
S (7,10)	525	242
S (7,11)	550	242
S (7,12)	575	242

Table 2. Case A. Sensors distribution and position. The coordinates have to be intended referred to the reference system present in Figure 4.

A.1 No failure (seepage analysis)

No relevant movements in the down stream slope are registered for an incoming discharge of

Q_{A1} = 25.46l/s.

Therefore the problem of evolution of the seepage line can be analyzed considering the dam as fixed.

The bottom pressure distribution is presented in Table 3.

Sensor	Pressure (cm)
S (1,1)	-
S (1,2)	-
S (1,3)	27.7
S (1,4)	24.1
S (1,5)	18.7
S (1,6)	5.0
S (1,7)	-
S (1,8)	-
S (1,9)	-
S (1,10)	-
S (1,11)	-
S (1,12)	-

Sensor	Pressure (cm)
S (4,1)	-
S (4,2)	-
S (4,3)	28.0
S (4,4)	24.1
S (4,5)	18.9
S (4,6)	4.5
S (4,7)	-
S (4,8)	-
S (4,9)	-
S (4,10)	-
S (4,11)	-
S (4,12)	-

Sensor	Pressure (cm)
S (7,1)	-
S (7,2)	-
S (7,3)	28.0
S (7,4)	24.0
S (7,5)	18.6
S (7,6)	3.7
S (7,7)	-
S (7,8)	-
S (7,9)	-
S (7,10)	-
S (7,11)	-
S (7,12)	-

Table 3. Case A.1. Bottom pressure heights at the steady state for an incoming discharge Q_{A1}.

A.2 Failure evolution

Increasing the incoming discharges the downstream slope starts to deform and a coupled problem should be considered.
Three sub cases are proposed and data of the stationary state of each one are provided.

A.2.1

Imposing an incoming discharge of

Q_{A21} = 51.75l/s

the downstream material starts to move and part of the toe of the dam starts to slip.

At the steady state the pressure distribution registered is the one presented in Table 4.

Sensor	Pressure (cm)
S (1,1)	-
S (1,2)	-
S (1,3)	43.1
S (1,4)	36.2
S (1,5)	24.2
S (1,6)	10.2
S (1,7)	-
S (1,8)	-
S (1,9)	-
S (1,10)	-
S (1,11)	-
S (1,12)	-

Sensor	Pressure (cm)
S (4,1)	-
S (4,2)	-
S (4,3)	43.1
S (4,4)	36.1
S (4,5)	24.9
S (4,6)	9.1
S (4,7)	-
S (4,8)	-
S (4,9)	-
S (4,10)	-
S (4,11)	-
S (4,12)	-

Sensor	Pressure (cm)
S (7,1)	-
S (7,2)	-
S (7,3)	43.5
S (7,4)	36.0
S (7,5)	24.7
S (7,6)	9.6
S (7,7)	-
S (7,8)	-
S (7,9)	-
S (7,10)	-
S (7,11)	-
S (7,12)	-

Table 4. Case A.2.1. Bottom pressure heights at the steady state for an incoming discharge Q_{A21}.

The advance degree of failure is

$$B = 71cm;$$

It is deduced from the digital model of the deformed slope shown in Figure 6.

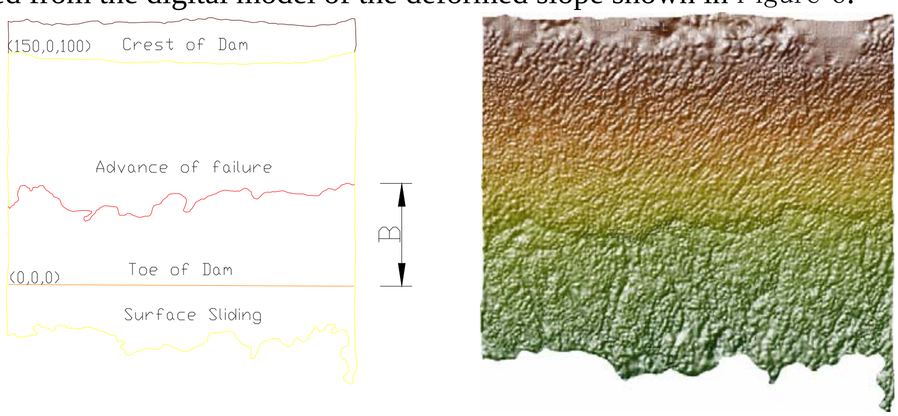

Figure 6. Case A.2.1. Digital model of the slope to evaluate the advance degree of failure B.

A.2.2

In the case of an incoming discharge

$$\boxed{Q_{A22} = 69.07 l/s}$$

the correspondent pressure distribution is given in Table 5.

Sensor	Pressure (cm)	Sensor	Pressure (cm)	Sensor	Pressure (cm)
S (1,1)	-	S (4,1)	-	S (7,1)	-
S (1,2)	-	S (4,2)	-	S (7,2)	-
S (1,3)	51.0	S (4,3)	51.0	S (7,3)	51.3
S (1,4)	41.5	S (4,4)	41.5	S (7,4)	41.4
S (1,5)	27.4	S (4,5)	28.1	S (7,5)	27.6
S (1,6)	13.0	S (4,6)	13.1	S (7,6)	13.6
S (1,7)	-	S (4,7)	-	S (7,7)	-
S (1,8)	-	S (4,8)	-	S (7,8)	-
S (1,9)	-	S (4,9)	-	S (7,9)	-
S (1,10)	-	S (4,10)	-	S (7,10)	-
S (1,11)	-	S (4,11)	-	S (7,11)	-
S (1,12)	-	S (4,12)	-	S (7,12)	-

Table 5. Case A.2.2. Bottom pressure heights at the steady state for an incoming discharge Q_{A22}.

The advance degree of failure for the present case is

$$B = 107.8cm;$$

and the digital model of the deformed slope is given in Figure 7.

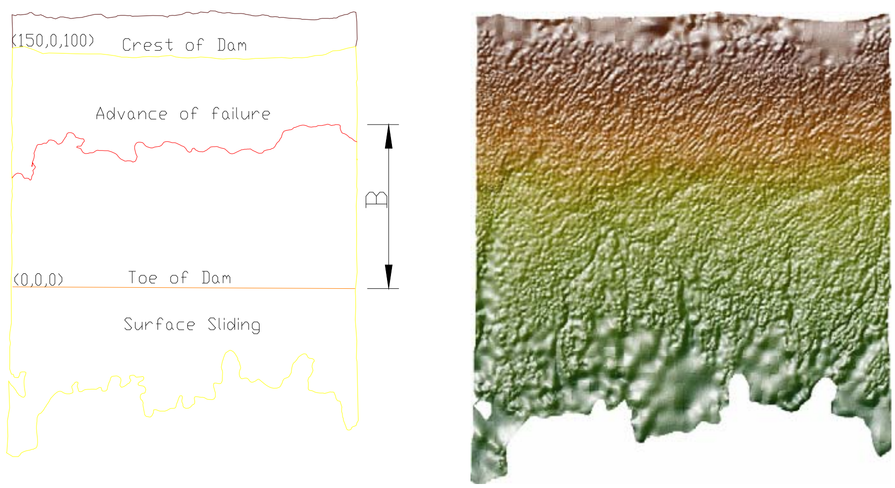

Figure 7. Case A.2.2. Digital model of the slope to evaluate the advance degree of failure B.

A.2.3

In the case of an incoming discharge

$$Q_{A23} = 90.68 l/s$$

the correspondent pressure distribution is given in Table 6.

Sensor	Pressure (cm)	Sensor	Pressure (cm)	Sensor	Pressure (cm)
S (1,1)	-	S (4,1)	-	S (7,1)	-
S (1,2)	-	S (4,2)	-	S (7,2)	-
S (1,3)	57.3	S (4,3)	57.4	S (7,3)	57.4
S (1,4)	45.2	S (4,4)	44.5	S (7,4)	44.8
S (1,5)	25.9	S (4,5)	26.1	S (7,5)	24.8
S (1,6)	19.6	S (4,6)	18.4	S (7,6)	20
S (1,7)	-	S (4,7)	-	S (7,7)	-
S (1,8)	-	S (4,8)	-	S (7,8)	-
S (1,9)	-	S (4,9)	-	S (7,9)	-
S (1,10)	-	S (4,10)	-	S (7,10)	-
S (1,11)	-	S (4,11)	-	S (7,11)	-
S (1,12)	-	S (4,12)	-	S (7,12)	-

Table 6. Case A.2.3. Bottom pressure heights at the steady state for an incoming discharge Q_{A23}.

The advance degree of failure for the present case is

$$B = 155.6\text{cm};$$

It is taken form the digital model of the downstream slope presented in Figure 8.

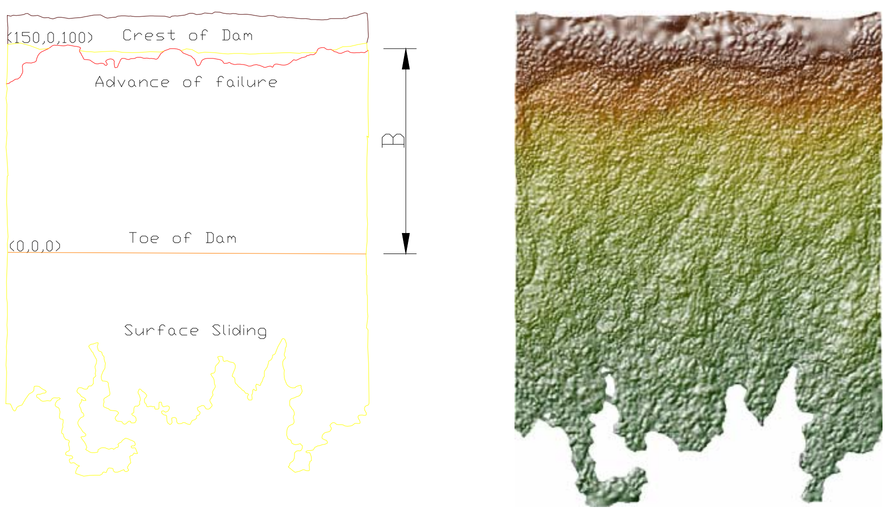

Figure 8. Case A.2.3. Digital model of the slope to evaluate the advance degree of failure B.

CASE B) CORE DAM

The second experiment that we propose is a core dam. In this particular case the core is considered rigid and its possible failure is not taken into account. The experiment was performed by UPM.

Geometry and material

The material used in this case is the same than in case A.

Porosity	= 0.4052;
Pore index	= 0.68;
Apparent specific weight	= 2.50 gr/cm^3
Dry density	= 1.49 gr/cm^3
Saturated density	= 1.91 gr/cm^3
D_{50}	= 35.04mm.

Where porosity is by definition the volume of empty space over the total volume and D_{50} is the mean diameter.

The geometrical setting of this experiment is described in Figure 9, where also the sensor distribution is given, nevertheless their coordinates are detailed also in Table 7.

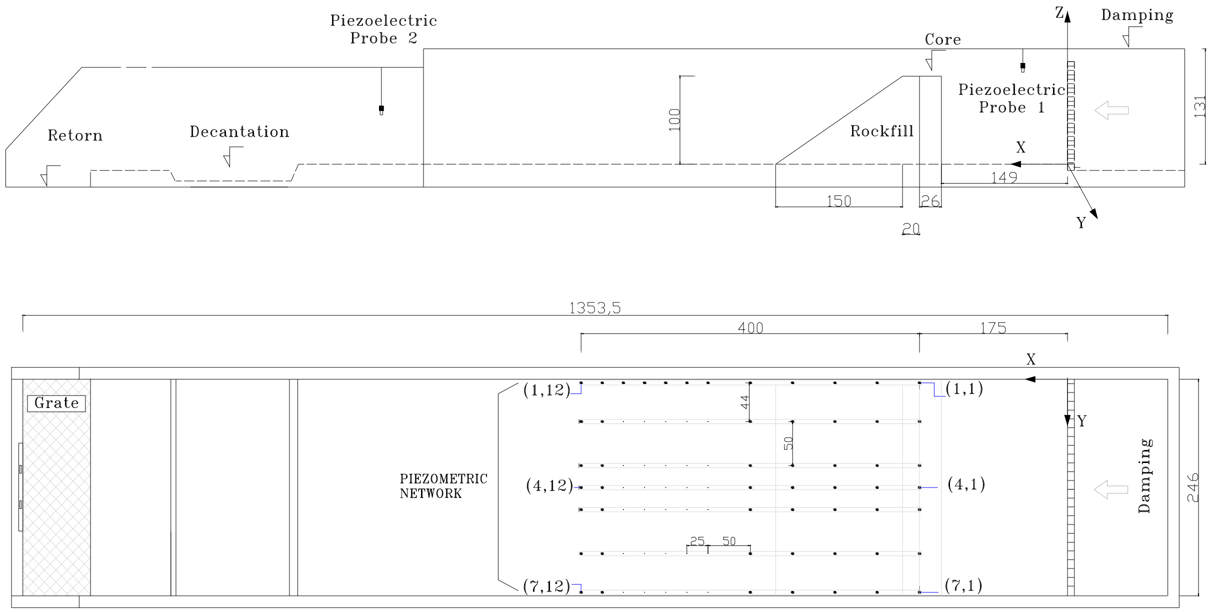

Figure 9. Case B. Geometry of the experimental setting and of the dam and pressure sensor distribution. All the measurements are in millimetres.

The experimental channel is the same than in Case A. The core dam is simulated reproducing only the downstream shoulder.

Sensor	X (cm)	Y (cm)
S (1,1)	175	4
S (1,2)	225	4
S (1,3)	275	4
S (1,4)	325	4
S (1,5)	375	4
S (1,6)	425	4
S (1,7)	450	4
S (1,8)	475	4
S (1,9)	500	4
S (1,10)	525	4
S (1,11)	550	4
S (1,12)	575	4

Sensor	X (cm)	Y (cm)
S (2,1)	175	48
S (2,2)	225	48
S (2,3)	275	48
S (2,4)	325	48
S (2,5)	375	48
S (2,6)	425	48
S (2,7)	450	48
S (2,8)	475	48
S (2,9)	500	48
S (2,10)	525	48
S (2,11)	550	48
S (2,12)	575	48

Sensor	X (cm)	Y (cm)
S (3,1)	175	98
S (3,2)	225	98
S (3,3)	275	98
S (3,4)	325	98
S (3,5)	375	98
S (3,6)	425	98
S (3,7)	450	98
S (3,8)	475	98
S (3,9)	500	98
S (3,10)	525	98
S (3,11)	550	98
S (3,12)	575	98

Sensor	X (cm)	Y (cm)
S (4,1)	175	123
S (4,2)	225	123
S (4,3)	275	123
S (4,4)	325	123
S (4,5)	375	123
S (4,6)	425	123
S (4,7)	450	123
S (4,8)	475	123
S (4,9)	500	123
S (4,10)	525	123
S (4,11)	550	123
S (4,12)	575	123

Sensor	X (cm)	Y (cm)
S (5,1)	175	148
S (5,2)	225	148
S (5,3)	275	148
S (5,4)	325	148
S (5,5)	375	148
S (5,6)	425	148
S (5,7)	450	148
S (5,8)	475	148
S (5,9)	500	148
S (5,10)	525	148
S (5,11)	550	148
S (5,12)	575	148

Sensor	X (cm)	Y (cm)
S (6,1)	175	198
S (6,2)	225	198
S (6,3)	275	198
S (6,4)	325	198
S (6,5)	375	198
S (6,6)	425	198
S (6,7)	450	198
S (6,8)	475	198
S (6,9)	500	198
S (6,10)	525	198
S (6,11)	550	198
S (6,12)	575	198

Sensor	X (cm)	Y (cm)
S (7,1)	175	242
S (7,2)	225	242
S (7,3)	275	242
S (7,4)	325	242
S (7,5)	375	242
S (7,6)	425	242
S (7,7)	450	242
S (7,8)	475	242
S (7,9)	500	242
S (7,10)	525	242
S (7,11)	550	242
S (7,12)	575	242

Table 7. Case B. Sensors distribution and position. The coordinates have to be intended referred to the reference system presented in Figure 9**.**

B.1 No failure (seepage analysis)

No relevant movements in the downstream slope are registered for an incoming discharge of

$$Q_{B1} = 5.93 l/s.$$

Therefore the problem of evolution of the seepage line can be analyzed considering the dam as fixed.

The bottom pressure distribution is presented in Table 8.

Sensor	Pres (cm)
S (1,1)	15.6
S (1,2)	14.0
S (1,3)	11.2
S (1,4)	3.2
S (1,5)	2.4
S (1,6)	2.4
S (1,7)	2.4
S (1,8)	2.4
S (1,9)	2.4
S (1,10)	2.4
S (1,11)	2.4
S (1,12)	2.4

Sensor	Pres (cm)
S (2,1)	15.6
S (2,2)	14
S (2,3)	11.2
S (2,4)	2.5
S (2,5)	2.4
S (2,6)	2.4
S (2,7)	2.4
S (2,8)	2.4
S (2,9)	2.4
S (2,10)	2.4
S (2,11)	2.4
S (2,12)	2.4

Sensor	Pres (cm)
S (3,1)	15.6
S (3,2)	14.0
S (3,3)	11.2
S (3,4)	2.9
S (3,5)	2.4
S (3,6)	2.4
S (3,7)	2.4
S (3,8)	2.4
S (3,9)	2.4
S (3,10)	2.4
S (3,11)	2.4
S (3,12)	2.4

Sensor	Pres (cm)
S (4,1)	15.6
S (4,2)	14.0
S (4,3)	11.2
S (4,4)	3.5
S (4,5)	2.4
S (4,6)	2.4
S (4,7)	2.4
S (4,8)	2.4
S (4,9)	2.4
S (4,10)	2.4
S (4,11)	2.4
S (4,12)	2.4

Sensor	Pres (cm)
S (5,1)	15.6
S (5,2)	14.0
S (5,3)	11.2
S (5,4)	2.9
S (5,5)	2.4
S (5,6)	2.4
S (5,7)	2.4
S (5,8)	2.4
S (5,9)	2.4
S (5,10)	2.4
S (5,11)	2.4
S (5,12)	2.4

Sensor	Pres (cm)
S (6,1)	15.6
S (6,2)	13.7
S (6,3)	11.2
S (6,4)	2.9
S (6,5)	2.4
S (6,6)	2.4
S (6,7)	2.4
S (6,8)	2.4
S (6,9)	2.4
S (6,10)	2.4
S (6,11)	2.4
S (6,12)	2.4

Sensor	Pres (cm)
S (7,1)	15.4
S (7,2)	13.5
S (7,3)	11.0
S (7,4)	2.7
S (7,5)	2.4
S (7,6)	2.4
S (7,7)	2.4
S (7,8)	2.4
S (7,9)	2.4
S (7,10)	2.4
S (7,11)	2.4
S (7,12)	2.4

Table 8. Case B.1. Bottom pressure heights at the steady state for an incoming discharge Q_{B1}.

B.2 Failure evolution

B.2.1

The second step of discharge is

$$Q_{B21} = 19.36 l/s$$

In this case the downstream slope starts to deform. Once a stable configuration is achieved, the pressure distribution is read and registered. It is detailed in Table 9.

Sensor	Pres (cm)
S (1,1)	33.6
S (1,2)	28.7
S (1,3)	21.4
S (1,4)	6.8
S (1,5)	4.0
S (1,6)	4.0
S (1,7)	4.0
S (1,8)	4.0
S (1,9)	4.0
S (1,10)	4.0
S (1,11)	4.0
S (1,12)	4.0

Sensor	Pres (cm)
S (2,1)	33.6
S (2,2)	28.7
S (2,3)	22.1
S (2,4)	7.0
S (2,5)	4.0
S (2,6)	4.0
S (2,7)	4.0
S (2,8)	4.0
S (2,9)	4.0
S (2,10)	4.0
S (2,11)	4.0
S (2,12)	4.0

Sensor	Pres (cm)
S (3,1)	33.6
S (3,2)	28.6
S (3,3)	22.1
S (3,4)	7.0
S (3,5)	4.0
S (3,6)	4.0
S (3,7)	4.0
S (3,8)	4.0
S (3,9)	4.0
S (3,10)	4.0
S (3,11)	4.0
S (3,12)	4.0

Sensor	Pres (cm)
S (4,1)	33.6
S (4,2)	28.6
S (4,3)	21.9
S (4,4)	6.8
S (4,5)	4.0
S (4,6)	4.0
S (4,7)	4.0
S (4,8)	4.0
S (4,9)	4.0
S (4,10)	4.0
S (4,11)	4.0
S (4,12)	4.0

Sensor	Pres (cm)
S (5,1)	33.3
S (5,2)	28.6
S (5,3)	21.5
S (5,4)	6.6
S (5,5)	4.0
S (5,6)	4.0
S (5,7)	4.0
S (5,8)	4.0
S (5,9)	4.0
S (5,10)	4.0
S (5,11)	4.0
S (5,12)	4.0

Sensor	Pres (cm)
S (6,1)	33.5
S (6,2)	28.4
S (6,3)	21.7
S (6,4)	6.5
S (6,5)	4.0
S (6,6)	4.0
S (6,7)	4.0
S (6,8)	4.0
S (6,9)	4.0
S (6,10)	4.0
S (6,11)	4.0
S (6,12)	4.0

Sensor	Pres (cm)
S (7,1)	33.1
S (7,2)	28.4
S (7,3)	21.2
S (7,4)	6.5
S (7,5)	4.0
S (7,6)	4.0
S (7,7)	4.0
S (7,8)	4.0
S (7,9)	4.0
S (7,10)	4.0
S (7,11)	4.0
S (7,12)	4.0

Table 9. Case B.2.1. Bottom pressure heights at the steady state for an incoming discharge Q_{B21}.

Figure 10. Case B.2.1 Steady state stable configuration achieved for a discharge Q_{B21}.

The advance degree of failure is measured visually. It is

$$B = 32 \text{ cm};$$

The stable deformed configuration of the downstream slope is shown in Figure 10.

B.2.2

In the case of an incoming discharge

$$\boxed{Q_{B22} = 30.45 \text{l/s}}$$

the pressure distribution at the stable configuration is given in Table 10.

Sensor	Pres (cm)
S (1,1)	41.6
S (1,2)	36.5
S (1,3)	25.0
S (1,4)	11.1
S (1,5)	4.8
S (1,6)	4.8
S (1,7)	4.8
S (1,8)	4.8
S (1,9)	4.8
S (1,10)	4.8
S (1,11)	4.8
S (1,12)	4.8

Sensor	Pres (cm)
S (2,1)	41.6
S (2,2)	36.5
S (2,3)	26.2
S (2,4)	10.3
S (2,5)	4.8
S (2,6)	4.8
S (2,7)	4.8
S (2,8)	4.8
S (2,9)	4.8
S (2,10)	4.8
S (2,11)	4.8
S (2,12)	4.8

Sensor	Pres (cm)
S (3,1)	41.7
S (3,2)	36.4
S (3,3)	26.1
S (3,4)	10.4
S (3,5)	4.8
S (3,6)	4.8
S (3,7)	4.8
S (3,8)	4.8
S (3,9)	4.8
S (3,10)	4.8
S (3,11)	4.8
S (3,12)	4.8

Sensor	Pres (cm)
S (4,1)	41.8
S (4,2)	36.5
S (4,3)	25.6
S (4,4)	10.4
S (4,5)	4.8
S (4,6)	4.8
S (4,7)	4.8
S (4,8)	4.8
S (4,9)	4.8
S (4,10)	4.8
S (4,11)	4.8
S (4,12)	4.8

Sensor	Pres (cm)
S (5,1)	41.4
S (5,2)	36.5
S (5,3)	25.1
S (5,4)	10.7
S (5,5)	4.8
S (5,6)	4.8
S (5,7)	4.8
S (5,8)	4.8
S (5,9)	4.8
S (5,10)	4.8
S (5,11)	4.8
S (5,12)	4.8

Sensor	Pres (cm)
S (6,1)	41.9
S (6,2)	36
S (6,3)	25.8
S (6,4)	9.8
S (6,5)	4.8
S (6,6)	4.8
S (6,7)	4.8
S (6,8)	4.8
S (6,9)	4.8
S (6,10)	4.8
S (6,11)	4.8
S (6,12)	4.8

Sensor	Pres (cm)
S (7,1)	41.5
S (7,2)	36.3
S (7,3)	25.3
S (7,4)	10.5
S (7,5)	4.8
S (7,6)	4.8
S (7,7)	4.8
S (7,8)	4.8
S (7,9)	4.8
S (7,10)	4.8
S (7,11)	4.8
S (7,12)	4.8

Table 10. Case B.2.2. Bottom pressure heights at the steady state for an incoming discharge Q_{B22}.

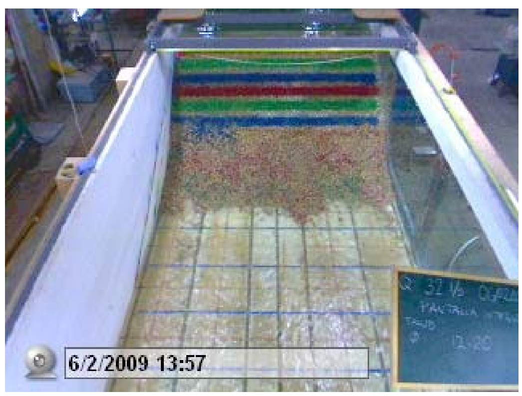

Figure 11. Case B.2.2 Steady state stable configuration achieved for a discharge Q_{B22}.

The advance degree of failure is measured visually. It is

$$B = 68cm;$$

The stable deformed configuration of the downstream slope is shown in Figure 11.

B.2.3

In the case of an incoming discharge

$$Q_{B23} = 39.56 l/s$$

the correspondent pressure distribution is given in Table 11.

Sensor	Pres (cm)
S (1,1)	46.9
S (1,2)	41.7
S (1,3)	27.7
S (1,4)	15.6
S (1,5)	5.3
S (1,6)	5.3
S (1,7)	5.3
S (1,8)	5.3
S (1,9)	5.3
S (1,10)	5.3
S (1,11)	5.3
S (1,12)	5.3

Sensor	Pres (cm)
S (2,1)	46.7
S (2,2)	41.6
S (2,3)	29.1
S (2,4)	14.4
S (2,5)	5.3
S (2,6)	5.3
S (2,7)	5.3
S (2,8)	5.3
S (2,9)	5.3
S (2,10)	5.3
S (2,11)	5.3
S (2,12)	5.3

Sensor	Pres (cm)
S (3,1)	46.7
S (3,2)	41.5
S (3,3)	29.1
S (3,4)	16.5
S (3,5)	5.3
S (3,6)	5.3
S (3,7)	5.3
S (3,8)	5.3
S (3,9)	5.3
S (3,10)	5.3
S (3,11)	5.3
S (3,12)	5.3

Sensor	Pres (cm)
S (4,1)	46.9
S (4,2)	41.5
S (4,3)	28.9
S (4,4)	17
S (4,5)	5.3
S (4,6)	5.3
S (4,7)	5.3
S (4,8)	5.3
S (4,9)	5.3
S (4,10)	5.3
S (4,11)	5.3
S (4,12)	5.3

Sensor	Pres (cm)
S (5,1)	46.3
S (5,2)	41.5
S (5,3)	28.2
S (5,4)	16.6
S (5,5)	5.3
S (5,6)	5.3
S (5,7)	5.3
S (5,8)	5.3
S (5,9)	5.3
S (5,10)	5.3
S (5,11)	5.3
S (5,12)	5.3

Sensor	Pres (cm)
S (6,1)	46.6
S (6,2)	40.7
S (6,3)	28.5
S (6,4)	15
S (6,5)	5.3
S (6,6)	5.3
S (6,7)	5.3
S (6,8)	5.3
S (6,9)	5.3
S (6,10)	5.3
S (6,11)	5.3
S (6,12)	5.3

Sensor	Pres (cm)
S (7,1)	46.4
S (7,2)	41.1
S (7,3)	27.4
S (7,4)	16.2
S (7,5)	5.3
S (7,6)	5.3
S (7,7)	5.3
S (7,8)	5.3
S (7,9)	5.3
S (7,10)	5.3
S (7,11)	5.3
S (7,12)	5.3

Table 11. Case B.2.3. Bottom pressure heights at the steady state for an incoming discharge Q_{B23}.

Figure 12. Case B.2.3 Steady state stable configuration achieved for a discharge Q_{B23}.

The advance degree of failure is measured visually. It is

$$B = 140.5cm;$$

The stable deformed configuration of the downstream slope is shown in Figure 12.

CASE C) IMPERMEABLE SCREEN DAM

The third and last case proposed is a dam with an impermeable upstream screen. This is experimentally simulated by a plastic fill that fully covers the upstream slope and it is glued to the side wall of the experimental channel. This experiment has been carried out by CEDEX.

Geometry and material

The geometry of the experimental setting is presented in Figure 13. The homogeneous material used in this case has the following characteristics:

Porosity	= 0.4052;
Pore index	= 0.68;
Apparent specific weight	= 2.50 gr/cm^3
Dry density	= 1.49 gr/cm^3
Saturated density	= 1.91 gr/cm^3
D_{50}	= 35.04mm.

The experimental setting and the sensor distribution is presented in Figure 13. The coordinates of these latter can be found in Table 12.

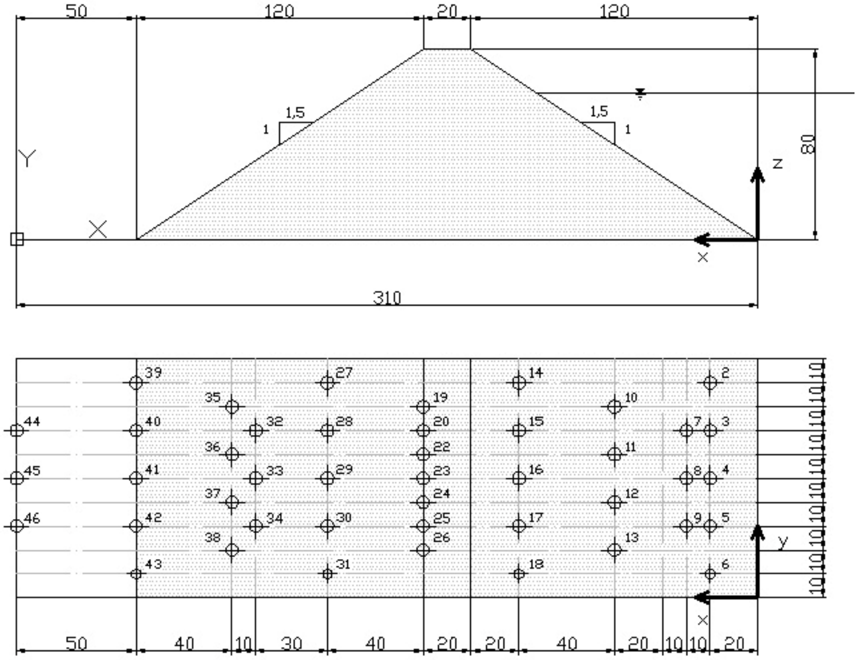

Figure 13. Case C. Geometry of the dam with impermeable screen in the upstream slope and position of the pressure sensors. All the dimensions have to be intended in cm.

Sensor	X position	Y position
2	20	90
3	20	70
4	20	50
5	20	30
6	20	10
7	30	70
8	30	50
9	30	30
10	60	80

Sensor	X position	Y position
11	60	60
12	60	40
13	60	20
14	100	90
15	100	70
16	100	50
17	100	30
18	100	10
19	140	80

Sensor	X position	Y position
20	140	70
22	140	60
23	140	50
24	140	40
25	140	30
26	140	20
27	180	90
28	180	70
29	180	50

Sensor	X position	Y position
30	180	30
31	180	10
32	210	70
33	210	50
34	210	30
35	220	80
36	220	60
37	220	40
38	220	20

Sensor	X position	Y position
39	260	90
40	260	70
41	260	50
42	260	30
43	260	10
44	310	70
45	310	50
46	310	30

Table 12. Case C. Sensors distribution and coordinates with respect to the global reference system presented in Figure 13.

C.1 No failure (seepage analysis)

Figure 14. Case C. Upper view of the dam.

$$Q_{C21} = 5.17 l/s$$

Sensor	Pressure
2	20.26cm
3	19.11cm
4	19.22cm
5	18.53cm
6	19.20cm
7	19.08cm
8	22.07cm
9	17.85cm
10	19.06cm

Sensor	Pressure
11	17.98cm
12	19.06cm
13	18.93cm
14	18.27cm
15	19.20cm
16	18.27cm
17	18.60cm
18	18.69cm
19	19.24cm

Sensor	Pressure
20	15.50cm
22	18.09cm
23	18.64cm
24	19.08cm
25	17.87cm
26	18.02cm
27	15.86cm
28	15.81cm
29	14.24cm

Sensor	Pressure
30	13.64cm
31	14.93cm
32	11.41cm
33	11.56cm
34	18.80cm
35	10.99cm
36	10.15cm
37	11.01cm
38	11.28cm

Sensor	Pressure
39	5.75cm
40	4.71cm
41	4.20cm
42	5.31cm
43	3.45cm
44	3.82cm
45	3.87cm
46	5.35cm

Table 13. Case C.1. Bottom pressure heights at the steady state for an incoming discharge Q_{C1}.

C.2 Failure evolution

C.2.1

The second step of discharge is

$$Q_{C21} = 15.36 l/s$$

In this case the downstream slope starts to deform. Once a stable configuration is achieved, the pressure distribution is read and registered. It is detailed in Table 14.

Sensor	Pressure
2	38.44 cm
3	36.39 cm
4	38.20 cm
5	37.27 cm
6	37.27 cm
7	36.81 cm
8	37.58 cm
9	37.25 cm
10	37.45 cm

Sensor	Pressure
11	37.25 cm
12	37.54 cm
13	37.16 cm
14	37.07 cm
15	37.14 cm
16	37.05 cm
17	36.92 cm
18	37.69 cm
19	36.28 cm

Sensor	Pressure
20	35.50 cm
22	35.50 cm
23	36.39 cm
24	36.08 cm
25	35.24 cm
26	35.48 cm
27	29.53 cm
28	29.55 cm
29	28.23 cm

Sensor	Pressure
30	28.74 cm
31	28.58 cm
32	22.50 cm
33	23.52 cm
34	26.26 cm
35	21.64 cm
36	19.73 cm
37	20.46 cm
38	20.46 cm

Sensor	Pressure
39	6.09 cm
40	6.51 cm
41	5.49 cm
42	6.62 cm
43	5.98 cm
44	6.05 cm
45	6.00 cm
46	5.67 cm

Table 14. Case C.2.1. Bottom pressure heights at the steady state for an incoming discharge Q_{C21}.

The advance degree of failure is measured with visual technique. It is

$$B_{C21} = 24cm;$$

C.2.2

In the case of an incoming discharge

$$\boxed{Q_{C22} = 25.05 l/s}$$

the correspondent pressure distribution is given in Table 15.

Sensor	Pressure
2	49.78 cm
3	49.23 cm
4	49.89 cm
5	48.90 cm
6	48.90 cm
7	48.97 cm
8	48.88 cm
9	48.75 cm
10	49.03 cm

Sensor	Pressure
11	48.77 cm
12	48.94 cm
13	48.88 cm
14	49.01 cm
15	49.12 cm
16	48.41 cm
17	48.28 cm
18	49.25 cm
19	47.44 cm

Sensor	Pressure
20	45.30 cm
22	45.81 cm
23	46.85 cm
24	46.67 cm
25	45.41 cm
26	44.68 cm
27	37.21 cm
28	36.66 cm
29	36.75 cm

Sensor	Pressure
30	36.57 cm
31	37.25 cm
32	25.85 cm
33	26.56 cm
34	30.21 cm
35	20.53 cm
36	21.34 cm
37	23.05 cm
38	21.10 cm

Sensor	Pressure
39	9.28 cm
40	10.14 cm
41	9.81 cm
42	10.52 cm
43	10.25 cm
44	7.49 cm
45	7.62 cm
46	7.60 cm

Table 15. Case C.2.1. Bottom pressure heights at the steady state for an incoming discharge Q_{C22}.

The advance degree of failure is measured with visual technique. It is

$$B_{C22} = 59.00cm;$$

C.2.3

In the case of an incoming discharge

$$\boxed{Q_{C23} = 30.27 l/s}$$

the correspondent pressure distribution is given in Table 16.

Sensor	Pressure
2	53.30 cm
3	52.73 cm
4	53.37 cm
5	52.42 cm
6	52.35 cm
7	52.66 cm
8	53.75 cm
9	52.58 cm
10	53.11 cm

Sensor	Pressure
11	52.60 cm
12	52.71 cm
13	52.40 cm
14	52.77 cm
15	53.33 cm
16	52.11 cm
17	51.91 cm
18	53.33 cm
19	50.94 cm

Sensor	Pressure
20	48.62 cm
22	48.77 cm
23	49.92 cm
24	50.14 cm
25	48.79 cm
26	48.44 cm
27	39.35 cm
28	30.82 cm
29	38.80 cm

Sensor	Pressure
30	39.22 cm
31	39.62 cm
32	29.00 cm
33	29.95 cm
34	32.98 cm
35	24.36 cm
36	25.17 cm
37	27.45 cm
38	25.77 cm

Sensor	Pressure
39	14.14 cm
40	15.05 cm
41	14.05 cm
42	15.80 cm
43	14.94 cm
44	8.72 cm
45	8.74 cm
46	8.59 cm

Table 16 .Case C.2.3. Bottom pressure heights at the steady state for an incoming discharge Q_{C23}

The advance degree of failure is measured with visual technique. It is

$$B_{C23} = 114.00cm.$$

ACKNOWLEDGEMENTS

The research was supported by the E-DAM project of the National Plan R+D of the Spanish Ministry of Science and Innovation I+D BIA2010-21350-C03-00.